

Article

Biofuels of Green Diesel–Kerosene–Gasoline Production from Palm Oil: Effect of Palladium Cooperated with Second Metal on Hydrocracking Reaction

Nithinun Srihanun ¹, Praepilas Dujjanutat ², Papasanee Muanruksa ^{1,3} and Pakawadee Kaewkannetra ^{4,5,*}

¹ Graduate School of Khon Kaen University, Khon Kaen 40002, Thailand; s.nithinun@gmail.com (N.S.); papasanee@gmail.com (P.M.)

² Postdoctoral Training of Department of Biotechnology, Khon Kaen University, Khon Kaen 40002, Thailand; praedujja@gmail.com

³ Department of Chemical Engineering and Analytical of Science (CEAS), The University of Manchester, Manchester M13 9PL, UK

⁴ Centre for Alternative Energy Research and Development (AERD), Faculty of Engineering, Khon Kaen University, Khon Kaen 40002, Thailand

⁵ Department of Biotechnology, Faculty of Technology, Khon Kaen University, Khon Kaen 40002, Thailand

* Correspondence: pakawadee.kku@gmail.com

Received: 8 January 2020; Accepted: 6 February 2020; Published: 18 February 2020



Abstract: In this work, two kinds of catalyst called monometallic Palladium (Pd) and a bimetallic of Pd-Iron (Fe) were synthesised using aluminum oxide (Al_2O_3) as the supported material via the wet impregnate method. A monometallic catalyst (0.5% Pd/ Al_2O_3) named Pd cat was used as control. For the bimetallic catalyst, ratios of Pd to Fe were varied, and included 0.38% Pd–0.12% Fe (PF1), 0.25% Pd–0.25% Fe (PF2), and 0.12% Pd–0.38% Fe (PF3). The catalysts were characterised to investigate physical properties such as the surface area, pore size, porosity, and pore size distribution including their composition by Brunauer–Emmett–Teller (BET) surface area, Scanning Electron Microscopy (SEM), and X-Ray Diffraction (XRD). Subsequently, all catalysts were applied for biofuels production in terms of green diesel/kerosene/gasoline from palm oil via a hydrocracking reaction. The results showed that the loading of Fe to Pd/ Al_2O_3 could improve the active surface area, porosity, and pore diameter. Considering the catalytic efficiency for the hydrocracking reaction, the highest crude biofuel yield (94.00%) was obtained in the presence of PF3 catalyst, while Pd cat provided the highest refined biofuel yield (86.00%). The largest proportion of biofuel production was green diesel (50.00–62.02%) followed by green kerosene (31.71–43.02%) and green gasoline (6.10–8.11%), respectively. It was clearly shown that the Pd-Fe bimetallic and Pd monometallic catalysts showed potential for use as chemical catalysts in hydrocracking reactions for biofuel production.

Keywords: Pd monometallic catalyst; Fe-Pd bimetallic catalysts; hydrocracking reaction; palm oil; green diesel; green kerosene; green gasoline

1. Introduction

The depletion of petroleum resources and its negative effect on the environment are the main inspiration for biofuel production from renewable sources [1]. Palm oils and its derivatives are one of the attractive biomasses for biofuel production due to their low cost and highest yield per hectare compared to other vegetable oils in Southeast Asia. Thailand is the third-largest palm oil producer in the world [2,3]. Recently, the hydroprocessing of triglycerides/fatty acid/fatty acid methyl ester

under high hydrogen pressure and temperature in the presence of catalyst is the most preferable for biofuel production [4]. In this process, unsaturated fatty acids are firstly converted into saturated fatty acids via hydrogenation followed by the hydrocracking of fatty acids into shorter chain hydrocarbon (C8–C16) through simultaneous reactions of decarboxylation/decarboxylation/hydrodeoxygenation.

There are many catalysts used for hydrocracking reaction such as nickel (Ni), niobium phosphate (NbOPO_4), zeolite, rhodium (Rh), platinum (Pt), and palladium (Pd). Among catalysts, noble metal catalysts (Pd and Pt) are the most favorable for hydrocracking reaction due to their high hydrogenation ability [5–8]. Previously, the comparison of catalytic efficiency between $\text{Pt/Al}_2\text{O}_3$ and $\text{Pd/Al}_2\text{O}_3$ catalysts for biofuels production from palm oil via hydrocracking reaction were studied by Dujjanutat et al. [9]. The results revealed that the highest biofuel yield (90%) was obtained with using $\text{Pd/Al}_2\text{O}_3$ catalyst, while $\text{Pt/Al}_2\text{O}_3$ presented a lower biofuel yield of 80%. Similarly, Choudhary et al. [10] also reported that Pd/C showed high efficiency for the deoxygenation of soybean oil with a total hydrocarbon content of 99%. The hydroprocessing of palm fatty acid distillate using Pd/C catalyst was also reported by Kiatkittipong et al. [11]. The highest diesel yield of 81% was obtained within 1 h. Although Pd catalyst showed high catalytic efficiency for biofuel production from triglycerides (TG), its high cost is the main limitation. As a result, the addition of low-cost active metal to monometallic Pd catalyst for bimetallic catalyst synthesis is an alternative approach to overcome this problem. However, to improve promoting catalytic activity, a secondary metal was added to cooperate with an active metal; this could enhance the stability of the resultant catalyst [12]. Iron (Fe) is one of low-cost active metals that has a reported highly desirable efficiency for hydrodeoxygenation [13]. Bimetallic Fe-Pd catalyst has ever been studied for various applications such as water gas shift [14], nitro reduction [15], the dechlorination of trichloroethene (TCE) in water [16] (Li et al., 2019), hydrogenation reaction [17,18] and hydrogenolysis for upgrading lignocellulosic material into valuable products [19,20]. As a result, it is interesting to apply Fe-Pd bimetallic catalyst for the hydrocracking of TG to produce valuable biofuels.

Moreover, the type of supporting material is also necessary according to surface area, porosity, and acidity, which are related to the conversion reaction and product selectivity. It seems that mesoporous materials offer moderate acidity, desired surface area, and pore sizes that are suitable for hydrocarbon fuel production. An oxide of alumina support (Al_2O_3) is the most popular mesoporous due to its high stability and moderate acidity. Acidic support can potentially break the C=O bond in fatty acid and perform hydrodeoxygenation reactions under temperatures less than 350 °C [21]. Accordingly, it is suitable for hydrocarbon fuel production in the ranges of green diesel and green kerosene using TG as feedstock. Furthermore, it also reported that it was the best support for Fe catalyst [13].

Therefore in this study, monometallic catalyst of $\text{Pd/Al}_2\text{O}_3$ and bimetallic catalyst of $\text{Fe-Pd/Al}_2\text{O}_3$ were synthesised in order to investigate their efficiency for biofuel production from palm oil via a hydrocracking reaction. The ratios of Fe and Pd loading for bimetallic catalyst synthesis was also investigated. The physical properties of catalysts were characterised to be the key that explained their catalytic performance. The metal dispersion of catalysts was studied by Scanning Electron Microscopy (SEM). The morphology of catalysts and the interaction between Pd and Fe were analysed by X-Ray Diffraction (XRD). The structural characteristics of catalysts including surface area, pore volume and pore diameter were investigated by the Brunauer–Emmett–Teller (BET) surface area technique. The catalytic testing of each catalyst was performed in a high-pressure batch reactor (HPBR). Finally, crude biofuel was separated to green diesel, green kerosene, and green gasoline via fractional distillation.

2. Results and Discussion

2.1. Composition of Palm Oil

Samples of refined palm oil (RPO) are characterised and presented in Table 1. Based on the fatty acids composition of RPO, it was found that the main compositions of RPO are palmitic acids (C16:0), palmitoleic acids (C16:1), stearic acids (C18:0), oleic acids (C18:1), and linoleic acids (C18:2).

Table 1. Fatty acids compositions of RPO.

Compositions	%wt.
Capric acid (C10:0)	0.11 ± 0.03
Lauric acid (C12:0)	1.58 ± 0.05
Myristic acid (C14:0)	4.74 ± 0.02
Palmitic acid (C16:0)	1.55 ± 0.01
Palmitoleic (C16:1)	12.50 ± 0.03
Stearic acid (C18:0)	1.82 ± 0.04
Oleic acid (C18:1)	76.27 ± 0.05
Linoleic acid (C18:2)	0.16 ± 0.06
Linolenic acid (C18:3)	0.08 ± 0.03
Arachidic acid (C20:0)	0.82 ± 0.06
Erucic acid (C22:1)	0.37 ± 0.04

2.2. Catalyst Characterisation

The BET data of a monometallic catalyst (0.5% Pd/Al₂O₃) named Pd cat, 0.38% Pd–0.12% Fe (PF1), 0.25% Pd–0.25% Fe (PF2), and 0.12% Pd–0.38% Fe (PF3) are demonstrated in Table 2. The PF3 catalyst showed the highest values of surface area (173.92 m²/g), pore volume (0.53 cm³/g), and pore diameter (9.27 nm). On the other hand, the lowest values of surface area (135.77 m²/g), pore volume (0.37 cm³/g), and pore diameter (8.13 nm) were observed for Pd cat. Both PF1 and PF2 catalysts showed similar results. It could be noted that high palladium loading caused a lower surface area, which was due to the agglomeration of the metallic particles [22]. Meanwhile, the addition of Fe could increase the specific surface area and reduce metallic particles [23].

Table 2. Physical properties of catalysts analysed by the Brunauer–Emmett–Teller (BET) method. PF1: 0.38% Pd–0.12% Fe, PF2: 0.25% Pd–0.25% Fe, PF3: 0.12% Pd–0.38% Fe.

Catalyst	BET Surface Area (m ² /g)	Pore Volume (cm ³ /g)	Ave. Pore Diameter (nm)
Pd cat	135.77 ± 0.05	0.37 ± 0.03	8.13 ± 0.06
PF1	157.32 ± 0.05	0.47 ± 0.05	9.10 ± 0.03
PF2	150.04 ± 0.03	0.48 ± 0.02	8.69 ± 0.04
PF3	173.92 ± 0.04	0.53 ± 0.04	9.27 ± 0.05

On the basis of nitrogen adsorption–desorption isotherms (See Figure 1), it was found that four catalysts (Pd cat, PF1, PF2, and PF3) presented relative pressure (P/P₀) curves at about 0.6–1.0. It indicated that all catalysts were classified as an H1 hysteresis loop with type IV set by the IUPAC (International Union of Pure and Applied Chemistry). Accordingly, there is an abundance of micropores and mesopores in their structure [7]. The advantages of mesoporous material include its moderate acidity, desirable specific surface area, and pore diameter, which is suitable for hydrocarbon fuel from triglycerides via hydrodeoxygenation reaction [21]. Furthermore, the pores diameter of mesoporous synthesized catalysts was proved that it can overcome the limitation diffusion of triglycerides [24].

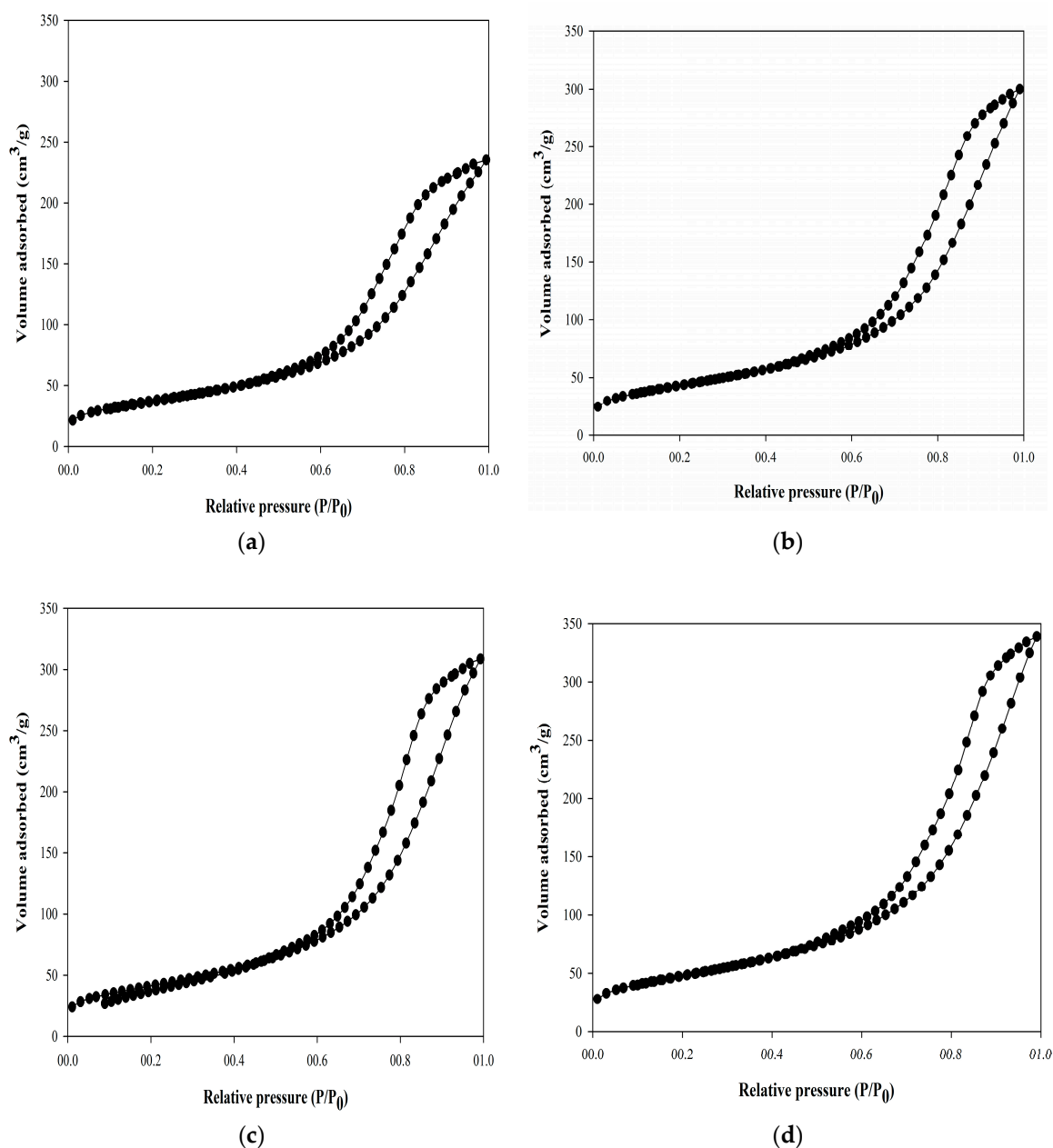


Figure 1. Curves of volume adsorbed (cm^3/g) as a function of relative pressure (P/P_0) for nitrogen sorption isotherms for mesoporous of (a) Pd cat, (b) PF1, (c) PF2, and (d) PF3 catalysts.

In Figure 2, SEM images of synthesised catalysts exhibited small particles of metal distribution on the surface area of the catalyst as well as on the supporting material. Meanwhile in Figure 3, an XRD technique was applied to identify a crystalline structure of all catalysts. The XRD pattern of the Pd cat, as well as the PF1, PF2, and PF3 catalysts are demonstrated in Figure 3. It was found that all monometallic/bimetallic catalysts clearly showed diffraction peaks of aluminum oxide (Al_2O_3). It was indicated that a supporting material of Al_2O_3 maintained its crystalline structure after Pd and Fe loading. A diffraction peak of a broad band centered at around 33° , corresponding to PdO. The peak of PdO was slightly distinct with a decreasing of Pd loading.

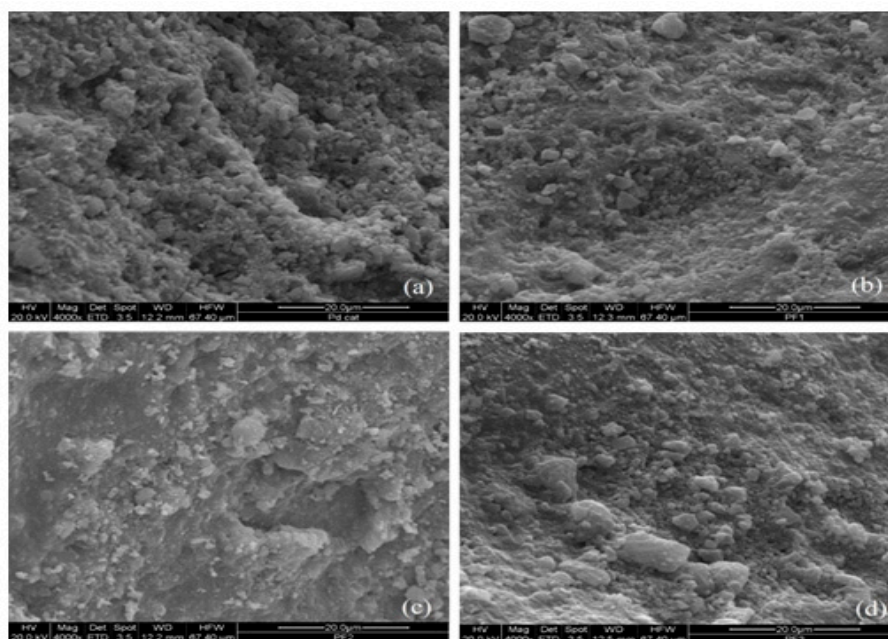


Figure 2. Scanning Electron Microscope (SEM) images of (a) Pd, (b) PF1, (c) PF2, and (d) PF3 catalysts ($\times 4000$ Magnification).

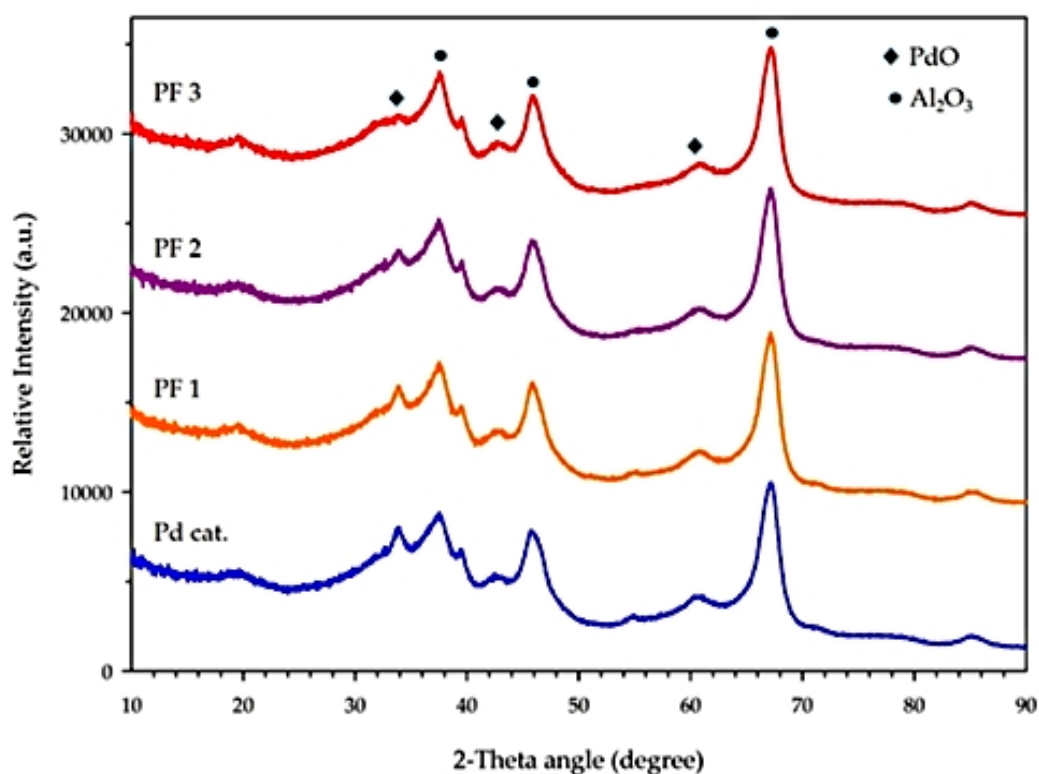


Figure 3. The XRD patterns (Pd cat, PF1, PF2, PF3) of PdO and Al_2O_3 catalysts analysed by X-ray diffractometer.

2.3. Catalytic Hydrocracking Reaction Test

The performance of Pd cat, PF1, PF2, and PF3 for biofuel production via hydrocracking reaction were investigated in HPBR. After the reaction, crude biofuel was distilled by a fractional distillater unit (ASTM D86) to obtain refined biofuel. The results of the crude-biofuel and refined-biofuel yields

are shown in Table 3. All catalysts could give a crude-biofuel yield in a range of 89–94%. The highest crude-biofuel yield of 94% was achieved in the presence of PF3 catalyst. It was due to loading Fe, which could increase the acidity and active site of catalyst, resulting in the high catalytic efficiency of catalyst [25]. It was in agreement with previous work [26] which reported that the loading of Fe-doped γ -Al₂O₃ catalyst exhibit enhanced catalytic activity due to higher Lewis acid sites. Denardin et al. [27] also reported that the addition of Fe onto HZSM-5 zeolite could increase the total acidity and strength of the strong acid sites. Monometallic catalyst (Pd cat) showed the highest catalytic efficiency for hydrocracking reaction with a high yield of refined biofuel (86%). For bimetallic catalysts, the refined biofuel percentages obtained from PF1, PF2, and PF3 were 74%, 66%, and 82%, respectively (see Figure 4). It should be noted that bimetallic catalysts showed a lower refined-biofuel yield than monometallic catalyst since the Fe catalyst increases olefin hydrocarbons including ethylene, propylene and butadiene better than refined-biofuel [13].

Table 3. Crude biofuel yield and valuable product obtained from catalytic hydrocracking reaction of monometallic and bimetallic catalysts.

Catalyst.	Metal Loading (wt.%)	Crude Biofuel Yield (%)	Refined Biofuel Yield (%)
Pd cat	0.5 Pd	91 ± 0.05	86 ± 0.03
PF1	0.38 Pd–0.12 Fe	89 ± 0.07	74 ± 0.05
PF2	0.25 Pd–0.25 Fe	92 ± 0.04	66 ± 0.04
PF3	0.12 Pd–0.38 Fe	94 ± 0.08	82 ± 0.02

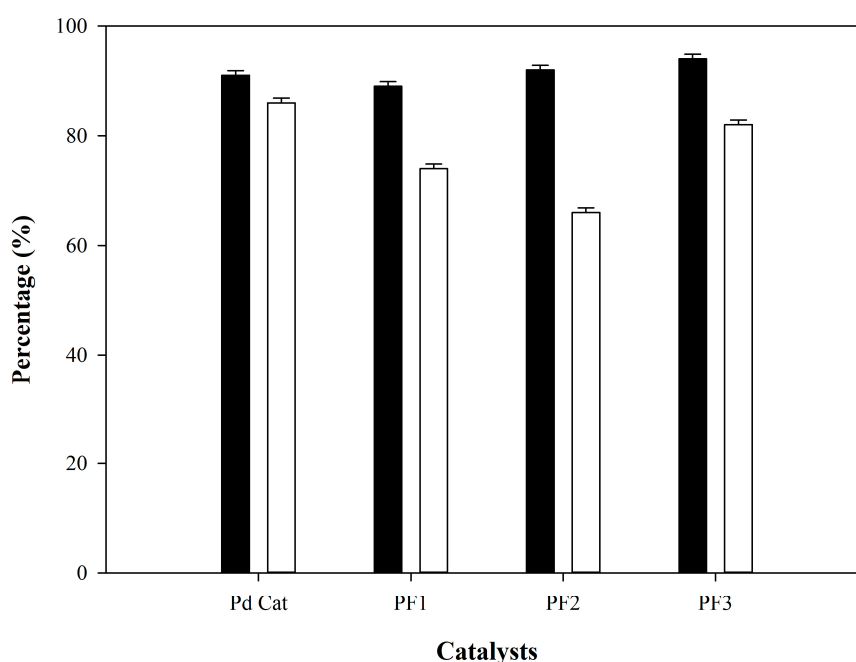


Figure 4. Crude-biofuel yield (■) and refined-biofuel yield (□) as function of different catalysts used (Pd cat, PF1, PF2, PF3).

Crude biofuels obtained from hydrocracking reaction could be classified into three kinds depending on their boiling point: (i) green gasoline, (ii) green kerosene, and (iii) green diesel, as illustrated in Figure 5. The highest diesel selectivity of 62.20% was obtained by using PF3 catalyst. Meanwhile, lower green diesel selectivity was observed in the cases of PF2 (56.06%) and PF1 (51.35%). Pd cat provided a diesel selectivity of 50%. The addition of Fe to monometallic Pd catalyst could increase the initial activity for the hydrodeoxygenation reaction, which was led to a higher diesel yield [28].

Considering kerosene selectivity, monometallic presented the highest kerosene selectivity of 43.02%. On the other hand, kerosene selectivity was slightly decreased in the presence of iron (Fe).

The kerosene selectivity of PF1, PF2, and PF3 was 40.54%, 36.36%, and 31.71%, respectively. This was in agreement with previous works [2,8,16], which reported that noble metal catalysts (Pd, Pt, Ni) could promote high kerosene selectivity via the hydrocracking reaction. Accordingly, Pd Cat could be considered as the best catalyst for kerosene production. In addition, green gasoline was also considered as the lowest selectivity (6.10–8.11%) for all catalysts.

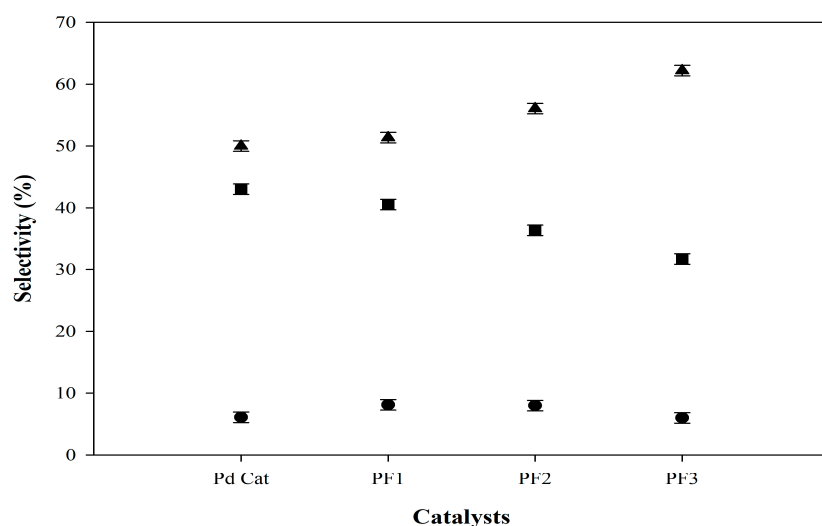


Figure 5. Percentage of selectivity in terms of green gasoline (●), green kerosene (■), and green diesel (▲) as functions of different catalysts (Pd cat, PF1, PF2, PF3).

Based on the results of refined biofuels, the largest proportion was green diesel followed by green kerosene and green gasoline, respectively. It was due to two main fatty acids of palmitic acid (C16:0) and oleic acid (C18:1) composed in palm oil. Carbon atoms of long chain fatty acid in palm oil were eliminated during the hydrocracking reaction through three different subreactions of (i) decarboxylation, (ii) decarbonylation, and (iii) hydrodeoxygenation. Meanwhile, carbon dioxide (CO₂), carbon monoxide (CO), and water (H₂O) were obtained as by-products. In Figure 6, oleic acid (C18:1) was converted into a hydrocarbon compound with 17–18 carbon atoms. If palmitic acid (C16:0) functioned as the substrate in the reaction, a hydrocarbon compound with 15–16 carbon atoms was obtained. Accordingly, the production of biofuel from palm oil via the hydrocracking reaction provided the most opportunity to obtain hydrocarbon fuel with carbon atoms (16–18), which was related to green diesel [7].

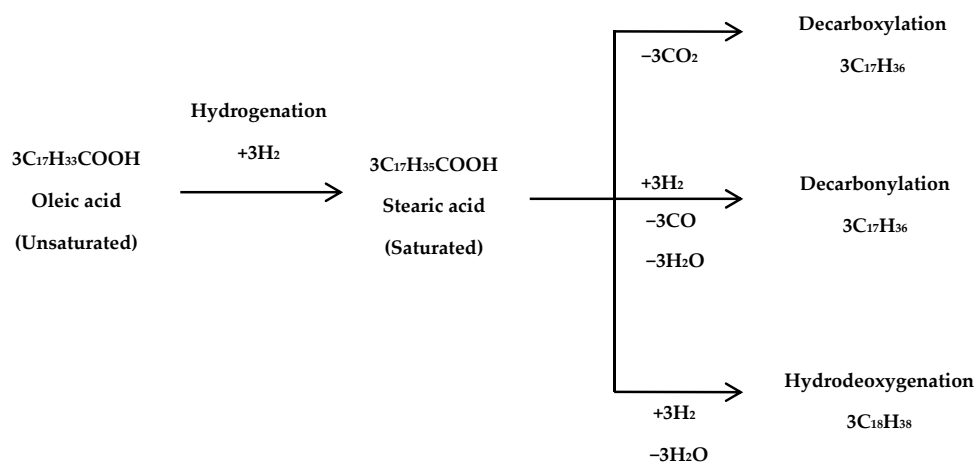


Figure 6. Simultaneous reactions of decarboxylation, decarbonylation, and hydrodeoxygenation of oleic acid.

2.4. Characterisation of Refined Biofuel Obtained from Hydrocracking Reaction

The carbon atom composition of refined biofuel was analyzed by gas chromatography (GC)-FID detector according to the UOP915 method. The result was found that carbon atom distribution was mainly in the range of green diesel (C15–C18), green kerosene (C9–C15), and green gasoline (C6–C9), respectively (see Figure 7).

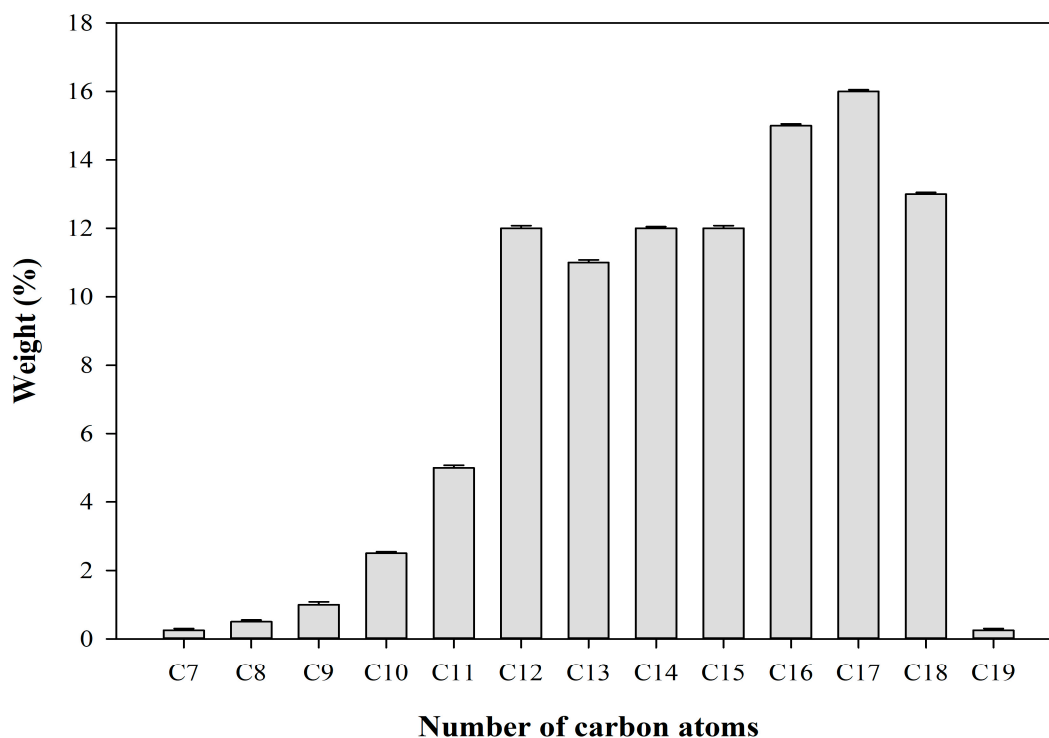


Figure 7. Number of carbon distribution of refined biofuel obtained from hydrocracking reaction (SD < 0.05).

2.5. Comparative Green Kerosene and Green Diesel Yields via Catalytic Cracking Reactions with Different Catalysts and Operating Conditions

According to the results shown in Table 4, both Pd monometallic and Pd-Fe bimetallic catalysts could provide high efficiency for biofuel production in the range of green kerosene/diesel via hydrocracking reaction, comparing to other previous works. It was interesting to note that the lowest catalyst loading was used for biofuel production from palm oil, but higher green kerosene/diesel yields were obtained for all four synthetic catalysts in this work. Only NbOPO₄ catalyst showed higher green kerosene yield than Pd/Pd-Fe catalysts. However, a high amount of NbOPO₄ (25%) and long reaction time (5 h) were used for green kerosene production from soybean oil [29]. Therefore, all synthetic catalysts (Pd Cat, PF1, PF2, and PF3) could be considered as high-efficiency chemical catalysts for biofuel production. Furthermore, we are the first group who attempted to investigate the catalytic hydrocracking reaction of Pd-Fe bimetallic catalysts for biofuel productions using palm oil as a raw material.

Table 4. Comparative green kerosene and green diesel yields via catalytic cracking reactions with different catalysts and operating conditions.

Feedstocks	Catalysts	Conditions	Green Kerosene Yield (%)	Green Diesel Yield (%)	Refs.
Palm oil	Pd Cat	0.9% catalyst, 400 °C, 60 bar H ₂ , 2 h	43.02	50.00	This work
Palm oil	PF1	0.9% catalyst, 400 °C, 60 bar H ₂ , 2 h	40.54	51.35	This work
Palm oil	PF2	0.9% catalyst, 400 °C, 60 bar H ₂ , 2 h	36.36	56.06	This work
Palm oil	PF3	0.9% catalyst, 400 °C, 60 bar H ₂ , 2 h	31.71	62.20	This work
Crude palm oil	5%Pd/C	5% catalyst, 400 °C, 40 bar H ₂ , 3 h	Not reported	51.00	[11]
Soybean oil	NbOPO ₄	25% catalyst, 350 °C, 10 bar H ₂ , 5 h	62.00	40.00	[29]
Coffee ground oil	5%Pd/C	5% catalyst, 400 °C, 40 bar H ₂ , 2 h	Not reported	22.30	[30]
Soybean	Pd-based zeolite	20% catalyst, 270 °C, 15 bar N ₂ , 1 h	31.00	Not reported	[31]
PFAD	Pd-based zeolite	20% catalyst, 270 °C, 15 bar N ₂ , 1 h	31.00	Not reported	[31]
Used lubricating oil	5%Fe/Al ₂ O ₃	4% catalyst, 450 °C, 6.8 bar H ₂ , 1.25 h	24.16	Not reported	[32]
Used lubricating oil	0.5%Fe/SiO ₂ -Al ₂ O ₃	4% catalyst, 430 °C, 6.8 bar H ₂ , 1 h	11.41	Not reported	[32]

3. Materials and Methods

3.1. Chemical Reagents

Chemical reagents are Pd (NO₃)₂·2H₂O and Fe(NO₃)₃·9H₂O including Al₂O₃ supporting material (3.8 nm average pore size, 45 nm particle size (TEM), 90 active acidic (0.063–0.200 mm) and 250 (m²/g) BET surface area) were purchased from Sigma-Aldrich chemical company, Bangkok Thailand. Palm oil was provided by Chumporn Palm Oil Industry, Thailand. Hydrogen gas with 95% purity was used as one of initial feedings during the reaction.

3.2. Characterisation of Palm Oil

The composition of palm oil was characterized according to method of the European Standard EN ISO 5509:2000. Firstly, palm oil (150 mg) and 0.5 M sodium hydroxide methanol solution (4 mL) were added into a 50-mL round-bottom flask and heated for 25 min. Subsequently, 5 mL of boron trifluoride (BF₃, approximately 1.3 M in methanol) was added and heated for 5 min. Isooctane (3 mL) was added into a mixture reaction. The mixture reaction was cooled down to room temperature and washed by saturated NaCl solution. The sample was injected to gas chromatography equipped with a flame ionization detector (GC-FID) to identify fatty acid composition.

3.3. Preparation of Supporting Material

Firstly, aluminum oxide (Al₂O₃) was prepared following the previous study explained by Srifa et al. [7]. The Al₂O₃ pellet was washed with deionised water twice. Then, it was dried at 120 °C in a hot air oven for 3 h. Finally, calcination of the Al₂O₃ pellet was carried out in a muffle furnace at 550 °C for 5 h in order to ensure morphological stability during the metal loading action. Both Pd (NO₃)₂·2H₂O and Fe (NO₃)₃·9H₂O were used as the metal precursors. The theoretical Pd and Fe loading were approximately 0.5% of the total metal based on the support with different weight, as demonstrated in Table 5.

Table 5. The amount of metals loading on Al₂O₃ support.

Catalysts	Metals Loading onto Al ₂ O ₃ Support (g)	
	Palladium (Pd)	Iron (Fe)
Pd cat	0.50	-
PF1	0.38	0.12
PF2	0.25	0.25
PF3	0.12	0.38

3.4. Monometallic Catalyst

The monometallic catalyst of palladium (Pd) was supported onto aluminum oxide (Al₂O₃) by the sequential incipient wetness impregnation method according to previous study [7]. Pd (0.5 g) was dissolved in deionised water and it subsequently was dropped into pretreated aluminum support (100 g) with continuous stirring at ambient temperature for 1 h. After that, the catalyst was dried at 100 °C in hot air oven for 12 h. Therefore, the impregnated catalyst was calcined in a muffle furnace at 550 °C for 5 h to obtain Pd cat.

3.5. Bimetallic Catalyst

Bimetallic catalysts of Pd and Fe were also prepared with different metals loadings, as shown in Table 2. Pd was first loaded on the support as previously described in Section 3.3 to obtain Pd cat. Then, the impregnation of an aqueous solution of Fe onto Pd/Al₂O₃ was carried out in a similar procedure. The sample was dried at 120 °C for 12 h and then calcined at 500 °C for 5 h to obtain PF1, PF2, and PF3.

3.6. Catalyst Characterisation

All catalysts used were characterised in a specific surface area and pore size distribution by the Brunauer–Emmett–Teller (BET) procedure using Micrometrics ASAP 2020 instrument (Micrometrics, Ottawa, ON, Canada) at −196 °C. Prior to the measurement, the catalyst was pretreated at 120 °C for 3 h [7]. The morphology and surface structure of the catalysts were characterised by using the scanning electron microscopy (SEM) (FEI Quanta 200, Thermo Fisher Scientific, Waltham, MA, USA). Meanwhile, the crystallographic phase of catalysts were verified by X-ray diffraction (XRD) peaks using X-ray diffractometer (PaNalytical X'pert Pro, Almelo, The Netherlands), under operating conditions of 40 kV, 40 mA using Cu K α radiation at $\lambda = 1.542 \text{ \AA}$ and increasing a step size of 0.0167° with a step time of 100 s in the range from 10° to 90°.

3.7. Hydrocracking Catalytic Reaction

The performances of catalysts in a hydrocracking reaction were performed in a high-pressure batch reactor (HPBR). Firstly, palm oil (100 mL) and catalyst (0.9 g) were loaded into the reactor. Then, hydrogen was fed to the reactor with an initial pressure at 60 bar, and the temperature was heated to 400 °C and held for 2 h. After the reaction, the reactor was allowed to cool down until room temperature. The crude biofuel was obtained and separated to green gasoline, green kerosene, and green diesel using standard fractional distillation (ASTM D86). The distilled biofuels were classified by different temperatures: green gasoline (50–150 °C), green kerosene (150–280 °C), and green diesel (280–360 °C). The crude-biofuel yield (%), refined-biofuel yield (%), green diesel selectivity (%), green kerosene selectivity (%), and green gasoline selectivity (%) were calculated as shown in Equations (1)–(5), respectively.

$$\% \text{ Crude-biofuel yield} = \frac{\text{Total crude biofuel (mL)}}{\text{Raw material (mL)}} \times 100\% \quad (1)$$

$$\% \text{ Refined-biofuel yield} = \frac{\text{Total biofuels obtained from distillation (mL)}}{\text{Total crude biofuel used in distillation (mL)}} \times 100\% \quad (2)$$

$$\% \text{ Green diesel selectivity} = \frac{\text{Green diesel obtained from distillation (mL)}}{\text{Total valuable product obtained from distillation (mL)}} \times 100\% \quad (3)$$

$$\% \text{ Green kerosene selectivity} = \frac{\text{Green kerosene obtained from distillation (mL)}}{\text{Total valuable product obtained from distillation (mL)}} \times 100\% \quad (4)$$

$$\% \text{ Green gasoline selectivity} = \frac{\text{Green gasoline obtained from distillation (mL)}}{\text{Total valuable product obtained from distillation (mL)}} \times 100\% \quad (5)$$

3.8. Characterisation of Refine -Biofuel Obtained from Hydrocracking Reaction

The refined biofuel was diluted 20 times with heptane. Then, a diluted sample (1 μL) was injected into the gas chromatography (GC) equipped with a flame ionization detector (FID). The carbon distribution of refined biofuel was analysed by GC-FID according to UOP 915 standard method.

4. Conclusions

Successfully, the synthesis of Pd monometallic/Pd-Fe bimetallic catalysts was carried out to apply for biofuels productions from palm oil. All catalysts were tested for catalytic hydrocracking reaction in HPBR under the same condition: 0.9 wt % catalyst loading, 400 °C reaction temperature, 40 bar initial H_2 pressure, and reaction time of 1 h. A high yield of both green kerosene (31.71–43.02%) and green diesel (50.00–62.20%) was obtained. It was indicated that the loading of low-cost metal (Fe) into Pd/ Al_2O_3 could improve the hydrocracking catalytic efficiency for biofuel production, especially regarding the selectivity of green diesel. Accordingly, the cooperation of a noble metal (Pd) and low-cost metal (Fe) on Al_2O_3 support could be considered as an alternative catalyst for low-cost biofuels production from renewable resources.

Author Contributions: This research article was conducted as collaboration among all authors. Methodology, resource, data curation and writing-original draft preparation, N.S. and P.D.; methodology, conceptualization, software, formal analysis and investigation, P.M.; validation and visualization and P.K.; supervision, project administration, funding acquisition and writing-review and editing. All authors have read and agree to the published version of the manuscript.

Funding: This research was co-funded by the Graduate School of Khon Kaen University, Khon Kaen, Thailand, (grant number 571T115 for N. Srihanun) and Post-Doctoral Training Program of Khon Kaen University, Khon Kaen, Thailand (grant number PD2563-07 for P. Dujjanutat).

Acknowledgments: All authors would like to sincerely and gratefully acknowledge for all of sponsors; Research grants from the Graduate School of Khon Kaen University and Post-Doctoral Training Program of Khon Kaen University, Khon Kaen, Thailand for co-funding. Department of Biotechnology, Faculty of Technology, Department of Chemical Engineering, Faculty of Engineering and Centre for Alternative Energy Research and Development (AERD), Khon Kaen University, Khon Kaen, Thailand for travel bursary, reactor, and partially fund. Chumporn Palm Oil Industry, Chumporn, Thailand for providing palm oil. In addition, The University of Manchester is also acknowledgment for experimental and analytical equipment support.

Conflicts of Interest: The authors declare no conflicts of interest.

References

1. Babaki, M.; Yousefi, M.; Habibi, Z.; Mohammadi, M. Process optimization for biodiesel production from waste cooking oil using multi-enzyme systems through response surface methodology. *Renew. Energy* **2017**, *105*, 465–472. [[CrossRef](#)]
2. Dujjanutat, P.; Kaewkannetra, P. Production of bio-hydrogenated kerosene by catalytic hydrocracking from refined bleached deodorised palm/ palm kernel oils. *Renew. Energy* **2020**, *147*, 464–472. [[CrossRef](#)]
3. Muanruksa, P.; Kaewkannetra, P. Combination of fatty acids extraction and enzymatic esterification for biodiesel production using sludge palm oil as a low-cost substrate. *Renew. Energy* **2020**, *146*, 901–906. [[CrossRef](#)]
4. Jeong, H.; Shin, M.; Jeong, B.; Jang, J.H.; Han, G.B.; Suh, Y.W. Comparison of activity and stability of supported Ni_2P and Pt catalysts in the hydro-processing of palm oil into normal paraffins. *J. Ind. Eng. Chem.* **2020**, *83*, 189–199. [[CrossRef](#)]

5. Anahas, A.M.P.; Muralitharan, G. Characterization of heterocystous cyanobacterial strains for biodiesel production based on fatty acid content analysis and hydrocarbon production. *Energy Convers. Manag.* **2018**, *157*, 423–437. [[CrossRef](#)]
6. Yang, L.; Carreon, M.A. Effect of reaction parameters on the decarboxylation of oleic acid over Pt/ZIF-67/membrane/zeolite 5A bead catalysts. *J. Chem. Technol. Biotechnol.* **2017**, *92*, 52–58. [[CrossRef](#)]
7. Srifa, A.; Faungnawakij, K.; Itthibenchapong, V.; Viriya-empikul, N.; Charinpanitkul, T.; Assabumrungrat, S. Production of bio-hydrogenated diesel by catalytic hydrotreating of palm oil over NiMoS₂/γ-Al₂O₃ catalyst. *Bioresour. Technol.* **2014**, *158*, 81–90. [[CrossRef](#)]
8. Dujjanutat, P.; Neramittagapong, A.; Kaewkannetra, P. Optimization of Bio-Hydrogenated Kerosene from Refined Palm Oil by Catalytic Hydrocracking. *Energies* **2019**, *12*, 3196. [[CrossRef](#)]
9. Dujjanutat, P.; Neramittagapong, A.; Kaewkannetra, P. H₂-Assisted Chemical Reaction for Green-Kerosene Production. *Defect Diffus. Forum* **2015**, *364*, 104–111. [[CrossRef](#)]
10. Choudhary, T.V.; Phillips, C.B. Renewable fuels via catalytic hydrodeoxygenation. *Appl. Catal. A Gen.* **2011**, *397*, 1–12. [[CrossRef](#)]
11. Kiatkittipong, W.; Phimsen, S.; Kiatkittipong, K.; Wongsakulphasatch, S.; Laosiripojana, N.; Assabumrungrat, S. Diesel-like hydrocarbon production from hydro-processing of relevant refining palm oil. *Fuel Process. Technol.* **2013**, *116*, 16–26. [[CrossRef](#)]
12. Xu, X.; Song, F.; Hu, X. A nickel iron diselenide-derived efficient oxygen-evolution catalyst. *Nat. Commun.* **2016**, *7*, 12324. [[CrossRef](#)]
13. Hwang, S.M.; Zhang, C.; Han, S.J.; Park, H.G.; Kima, Y.T.; Yang, S.; Jun, K.W.; Kim, S.K. Mesoporous carbon as an effective support for Fe catalyst for CO₂ hydrogenation to liquid hydrocarbons. *J. CO₂ Util.* **2020**, *37*, 65–73. [[CrossRef](#)]
14. Wang, X.; Gorte, R.J. The effect of Fe and other promoters on the activity of Pd/ceria for the water-gas shift reaction. *Appl. Catal. A Gen.* **2003**, *247*, 157–162. [[CrossRef](#)]
15. Metin, Ö.; Mendoza-Garcia, A.; Dalmizrak, D.; Gültekin, M.S.; Sun, S. FePd alloy nanoparticles assembled on reduced graphene oxide as a catalyst for selective transfer hydrogenation of nitroarenes to anilines using ammonia borane as a hydrogen source. *Catal. Sci. Technol.* **2016**, *6*, 6137–6143. [[CrossRef](#)]
16. Li, B.; Chen, X.; Li, K.; Zhang, C.; He, Y.; Du, R.; Wang, J.; Chen, L. Coupling membrane and Fe–Pd bimetallic nanoparticles for trichloroethene removing from water. *J. Ind. Eng. Chem.* **2019**, *78*, 198–209. [[CrossRef](#)]
17. Cheng, Y.; Pham, H.; Huo, J.; Johnson, R.; Datye, A.K.; Shanks, B. High activity Pd-Fe bimetallic catalysts for aqueous phase hydrogenations. *Mol. Catal.* **2019**, *477*, 110546. [[CrossRef](#)]
18. Cen, Y.; Yue, Y.; Wang, S.; Lu, J.; Wang, B.; Jin, C.; Guo, L.; Hu, Z.T.; Zhao, J. Adsorption Behavior and Electron Structure Engineering of Pd-Based Catalysts for Acetylene Hydrochlorination. *Catalysts* **2020**, *10*, 24. [[CrossRef](#)]
19. Espro, C.; Gumina, B.; Paone, E.; Mauriello, F. Upgrading lignocellulosic biomasses: Hydrogenolysis of platform derived molecules promoted by heterogeneous Pd-Fe catalysts. *Catalysts* **2017**, *7*, 78. [[CrossRef](#)]
20. Malara, A.; Paone, E.; Bonaccorsi, L.; Mauriello, F.; Macario, A.; Frontera, P. Nanofibers for the Catalytic Conversion of Lignin-Derived Benzyl Phenyl Ether under Transfer Hydrogenolysis Conditions. *Catalysts* **2020**, *10*, 20. [[CrossRef](#)]
21. Arun, N.; Sharma, R.V.; Dalai, A.K. Green diesel synthesis by hydrodeoxygenation of bio-based feedstocks: Strategies for catalyst design and development. *Renew. Sustain. Energy Rev.* **2015**, *48*, 240–255. [[CrossRef](#)]
22. Long, Y.; Liang, K.; Niu, J.; Tong, X.; Yuan, B.; Ma, J. Agglomeration of Pd⁰ nanoparticles causing different catalytic activities of Suzuki carbonylative cross-coupling reactions catalyzed by Pd^{II} and Pd⁰ immobilized on dopamine-functionalized magnetite nanoparticles. *New J. Chem.* **2015**, *39*, 2988–2996. [[CrossRef](#)]
23. Lyu, D.; Mollamahale, Y.B.; Huang, S.; Zhu, P.; Zhang, X.; Du, Y.; Wang, S.; Qing, M.; Tian, Z.Q.; Shen, P.K. Ultra-high surface area graphitic Fe-N-C nanospheres with single-atom iron sites as highly efficient non-precious metal bifunctional catalysts towards oxygen redox reactions. *J. Catal.* **2018**, *368*, 279–290. [[CrossRef](#)]
24. Ooi, X.Y.; Oi, L.E.; Choo, M.Y.; Ong, H.C.; Lee, H.V.; Show, P.L.; Lin, Y.C.; Juan, J.C. Efficient deoxygenation of triglycerides to hydrocarbon-biofuel over mesoporous Al₂O₃-TiO₂ catalyst. *Fuel Process. Technol.* **2019**, *194*, 106120. [[CrossRef](#)]
25. Cheng, S.; Wei, L.; Julson, J.; Rabnawaz, M. Upgrading pyrolysis bio-oil through hydro-deoxygenation (HDO) using non-sulfided Fe-Co/SiO₂ catalyst. *Energy. Convers. Manag.* **2017**, *150*, 331–342. [[CrossRef](#)]

26. Zhao, W.; Zheng, X.; Liang, S.; Zheng, X.; Shen, L.; Liu, F.; Cao, Y.; Wei, Z.; Jiang, L. Fe-doped γ - Al_2O_3 porous hollow microspheres for enhanced oxidative desulfurization: Facile fabrication and reaction mechanism. *Green Chem.* **2018**, *20*, 4645–4654. [[CrossRef](#)]
27. Denardin, F.; Perez-Lopez, O.W. Tuning the acidity and reducibility of Fe/ZSM-5 catalysts for methane dehydroaromatization. *Fuel* **2019**, *236*, 1293–1300. [[CrossRef](#)]
28. Kwon, E.E.; Kim, Y.T.; Kim, H.J.; Andrew Lin, K.Y.; Kim, K.H.; Lee, J.; Huber, G.W. Production of high-octane gasoline via hydrodeoxygenation of sorbitol over palladium-based bimetallic catalysts. *J. Environ. Manage.* **2018**, *227*, 329–334. [[CrossRef](#)]
29. Scaldaferrì, C.A.; Pasa, V.M.D. Production of jet fuel and green diesel range biohydrocarbons by hydro-processing of soybean oil over niobium phosphate catalyst. *Fuel* **2019**, *245*, 458–466. [[CrossRef](#)]
30. Phimsen, S.; Kiatkittipong, W.; Yamada, H.; Tagawa, T.; Kiatkittipong, K.; Laosiripojana, N.; Assabumrungrat, S. Oil extracted from spent coffee grounds for bio-hydrotreated diesel production. *Energy Convers. Manag.* **2016**, *126*, 1028–1036. [[CrossRef](#)]
31. Choi, I.H.; Hwang, K.R.; Han, J.S.; Lee, K.H.; Yun, J.S.; Lee, J.S. The direct production of jet-fuel from non-edible oil in a single-step process. *Fuel* **2015**, *158*, 98–104. [[CrossRef](#)]
32. Makvisai, W.; Promdee, K.; Tanatavikorn, H.; Vitidsant, T. Catalytic cracking of used lubricating oil over Fe/ Al_2O_3 and Fe/ SiO_2 - Al_2O_3 . *Pet. Coal* **2016**, *58*, 83–94.



© 2020 by the authors. Licensee MDPI, Basel, Switzerland. This article is an open access article distributed under the terms and conditions of the Creative Commons Attribution (CC BY) license (<http://creativecommons.org/licenses/by/4.0/>).